9-20-2016

MLKL and FADD Are Critical for Suppressing Progressive Lymphoproliferative Disease and Activating the NLRP3 Inflammasome.

Xixi Zhang
University of Chinese Academy of Sciences

Cunxian Fan
University of Chinese Academy of Sciences

Haiwei Zhang
University of Chinese Academy of Sciences

Qun Zhao
University of Chinese Academy of Sciences

ngbo Liu
University of Chinese Academy of Sciences

See next page for additional authors

Article

Cell Reports

MLKL and FADD Are Critical for Suppressing Progressive Lymphoproliferative Disease and Activating the NLRP3 Inflammasome

Graphical Abstract

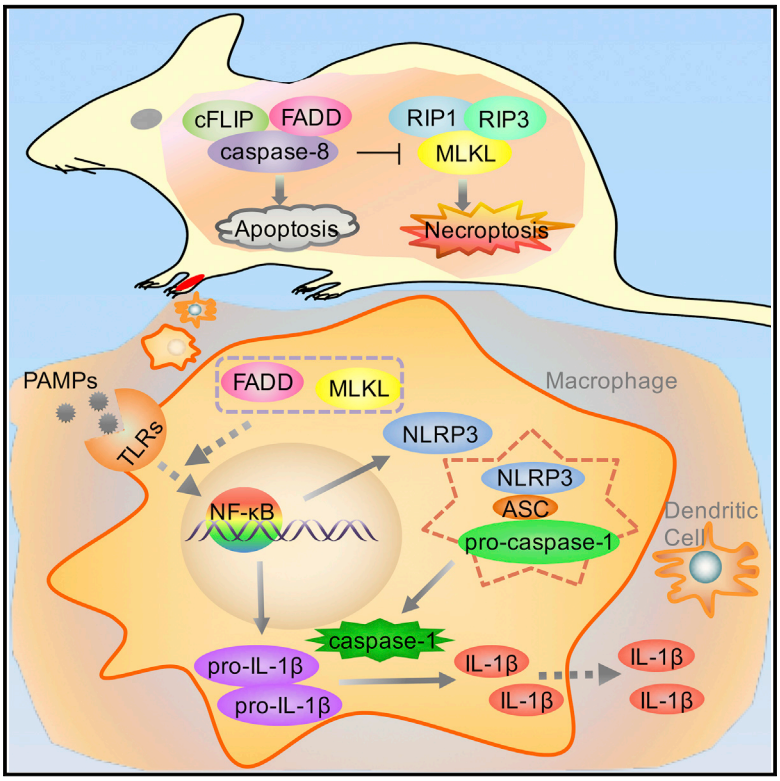

Highlights

- Ablation of *Mlkl* rescues embryonic lethality in *Fadd*-deficient mice
- *Mlkl*$^{-/-}$*Fadd*$^{-/-}$ mice show severe lymphoproliferative disease
- *Mlkl*$^{-/-}$*Fadd*$^{-/-}$ BMDMs and BMDCs have impaired NLRP3 inflammasome activation
- MLKL and FADD regulate ASC speck formation and NF-κB-dependent NLRP3 transcription

Authors

Xixi Zhang, Cunxian Fan, Haiwei Zhang, ..., Xianjun Yu, Jianke Zhang, Haibing Zhang

Correspondence

hbzhang@sibs.ac.cn

In Brief

Zhang et al. find that RIPK3-MLKL-mediated signaling results in embryonic lethality in *Fadd*-deficient mice. *Mlkl*$^{-/-}$*Fadd*$^{-/-}$ mice have more severe lymphoproliferative disease than *Fadd*$^{-/-}$*Ripk3*$^{-/-}$ mice. Further studies reveal that MLKL and FADD are critical for activating the NLRP3 inflammasome through regulation of ASC speck formation and NF-κB-dependent NLRP3 transcription.

Zhang et al., 2016, Cell Reports *16*, 3247–3259
September 20, 2016
http://dx.doi.org/10.1016/j.celrep.2016.06.103

Cell Reports
Article

MLKL and FADD Are Critical for Suppressing Progressive Lymphoproliferative Disease and Activating the NLRP3 Inflammasome

Xixi Zhang,[1,5] Cunxian Fan,[1,5] Haiwei Zhang,[1] Qun Zhao,[1] Yongbo Liu,[1] Chengxian Xu,[1] Qun Xie,[1,2] Xiaoxia Wu,[1] Xianjun Yu,[1,3] Jianke Zhang,[4] and Haibing Zhang[1,*]

[1]Key Laboratory of Nutrition and Metabolism, Institute for Nutritional Sciences, Shanghai Institutes for Biological Sciences, Chinese Academy of Sciences, University of Chinese Academy of Sciences, Shanghai 200031, China
[2]Department of Anesthesiology, Changhai Hospital, Second Military Medical University, Shanghai 200433, China
[3]Department of Biochemistry, Hubei University of Medicine, Shiyan 442000, China
[4]Department of Microbiology and Immunology, Sidney Kimmel Cancer Center, Sidney Kimmel Medical College, Thomas Jefferson University, Philadelphia, PA 19107, USA
[5]Co-first author
*Correspondence: hbzhang@sibs.ac.cn
http://dx.doi.org/10.1016/j.celrep.2016.06.103

SUMMARY

MLKL, a key component downstream of RIPK3, is suggested to be a terminal executor of necroptosis. Genetic studies have revealed that *Ripk3* ablation rescues embryonic lethality in *Fadd*- or *Caspase-8*-deficient mice. Given that RIPK3 has also been implicated in non-necroptotic pathways including apoptosis and inflammatory signaling, it remains unclear whether the lethality in *Fadd*$^{-/-}$ mice is indeed caused by necropotosis. Here, we show that genetic deletion of *Mlkl* rescues the developmental defect in *Fadd*-deficient mice and that *Fadd*$^{-/-}$*Mlkl*$^{-/-}$ mice are viable and fertile. *Mlkl*$^{-/-}$*Fadd*$^{-/-}$ mice display significantly accelerated lymphoproliferative disease characterized by lymphadenopathy and splenomegaly when compared to *Ripk3*$^{-/-}$ *Fadd*$^{-/-}$ mice. *Mlkl*$^{-/-}$*Fadd*$^{-/-}$ bone-marrow-derived macrophages and dendritic cells have impaired NLRP3 inflammasome activation associated with defects in ASC speck formation and NF-κB-dependent NLRP3 transcription. Our findings reveal that MLKL and FADD play critical roles in preventing lymphoproliferative disease and activating the NLRP3 inflammasome.

INTRODUCTION

Regulated cell death including apoptosis and necroptosis plays essential roles in the development, homeostasis, and pathological processes of mammals. Apoptosis can be triggered through the death receptors (DRs), including tumor necrosis factor receptor-1 (TNFR1) and FAS (Nagata, 1997). Activated by their ligands, DRs recruit the adaptor protein Fas-associated death domain (FADD), which binds and activates caspase-8 to initiate apoptosis (Boldin et al., 1996; Muzio et al., 1996; Zhang and Winoto, 1996). In the absence of active caspase-8, receptor-interacting protein kinase 1 (RIPK1) and RIPK3 interact with each other, forming a microfilament-like complex that is known as necrosome (Li et al., 2012; Orozco et al., 2014; Vercammen et al., 1998). MLKL, the mixed lineage kinase domain-like protein, has been identified as a key component downstream of RIPK3 (Sun et al., 2012; Zhao et al., 2012). Recent studies have demonstrated that MLKL is phosphorylated by RIPK3 and form oligomers that translocate to cell membrane, leading to the disruption of membrane integrity (Cai et al., 2014; Chen et al., 2014; Dondelinger et al., 2014; Orozco et al., 2014; Su et al., 2014; Wang et al., 2014).

The in vivo mechanism of RIPK1-RIPK3 necrosome-mediated necroptosis has been elucidated through intensive genetic studies. Targeted deletion of *Fadd* or *Caspase-8* in mice causes embryonic lethality around embryonic day 11.5 (Varfolomeev et al., 1998; Yeh et al., 1998), which is probably due to vascular, cardiac, and hematopoietic defects (Kang et al., 2004, 2008; Sakamaki et al., 2002). The death of *Fadd*$^{-/-}$ or *Casp8*$^{-/-}$ embryo can be rescued by co-deletion of *Ripk1*; however, similar to *Ripk1*$^{-/-}$ mice, these mice die perinatally (Zhang et al., 2011; Rickard et al., 2014; Dillon et al., 2014; Kaiser et al., 2014; Kelliher et al., 1998). Deletion of *Ripk3* in *Fadd*$^{-/-}$ or *Casp8*$^{-/-}$ mice also prevents the embryonic lethality (Dillon et al., 2012; Kaiser et al., 2011; Oberst et al., 2011); by contrast, *Ripk3*$^{-/-}$*Fadd*$^{-/-}$ and *Ripk3*$^{-/-}$*Casp8*$^{-/-}$ mice grow into fertile adults. Furthermore, co-deletion of *Ripk3* and either *Fadd* or *Caspase-8* can rescue *Ripk1*$^{-/-}$ mice into adulthood (Rickard et al., 2014; Dillon et al., 2014; Kaiser et al., 2014; Dowling et al., 2015). During necroptosis, the pseudokinase MLKL acts as a terminal executor downstream of necrosome formation. Thus, the strong evidence regarding the early embryonic death of *Fadd* or *Caspase-8*-deficient mice caused by RIPK3-dependent necroptosis could come from investigating putative MLKL functions in the *Fadd* or *Caspase-8*-deficient background.

Although the mice deficient in both *Fadd* and *Ripk3* are viable, they display a profound lymphoproliferative disease over time with a large accumulation of B220^{+} CD3^{+} T lymphocytes. Similar phenomena are observed in *Ripk3*$^{-/-}$*Casp8*$^{-/-}$ mice and *Ripk3*$^{D161N/D161N}$*Casp8*$^{-/-}$ mice (Dillon et al., 2012; Kaiser et al.,

A

B

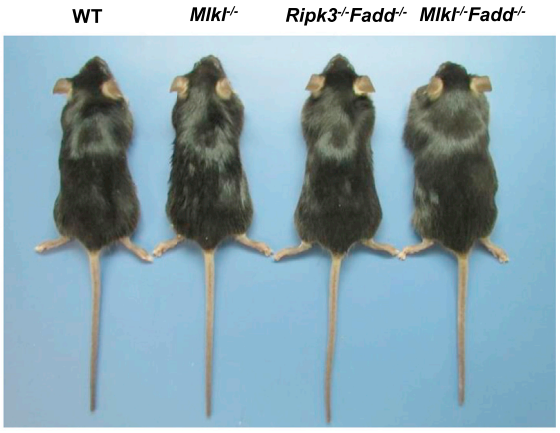

C

Mlkl$^{+/-}$*Fadd*$^{+/-}$ intercross

Genotype	Mendelian frequency(%)	Observed frequency(%)	Number of mice
Fadd$^{+/+}$*Mlkl*$^{+/+}$	6.25	8.57	12
Fadd$^{+/+}$*Mlkl*$^{+/-}$	12.5	5.71	8
Fadd$^{+/+}$*Mlkl*$^{-/-}$	6.25	12.86	18
Fadd$^{+/-}$ *Mlkl*$^{+/+}$	12.5	22.86	32
Fadd$^{+/-}$ *Mlkl*$^{+/-}$	25	25.71	36
Fadd$^{+/-}$ *Mlkl*$^{-/-}$	12.5	18.57	26
Fadd$^{-/-}$ *Mlkl*$^{+/+}$	6.25	0†	0†
Fadd$^{-/-}$ *Mlkl*$^{+/-}$	12.5	0†	0†
Fadd$^{-/-}$ *Mlkl*$^{-/-}$	6.25	5.71	8
		Total	140

D

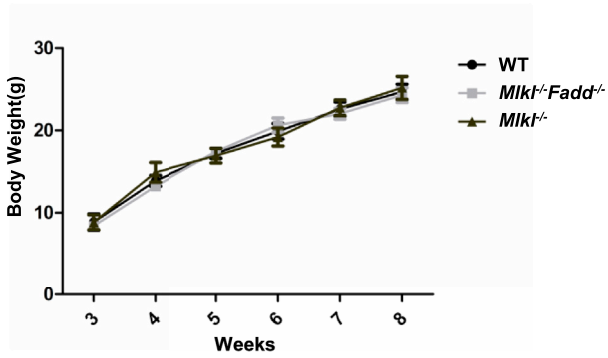

E

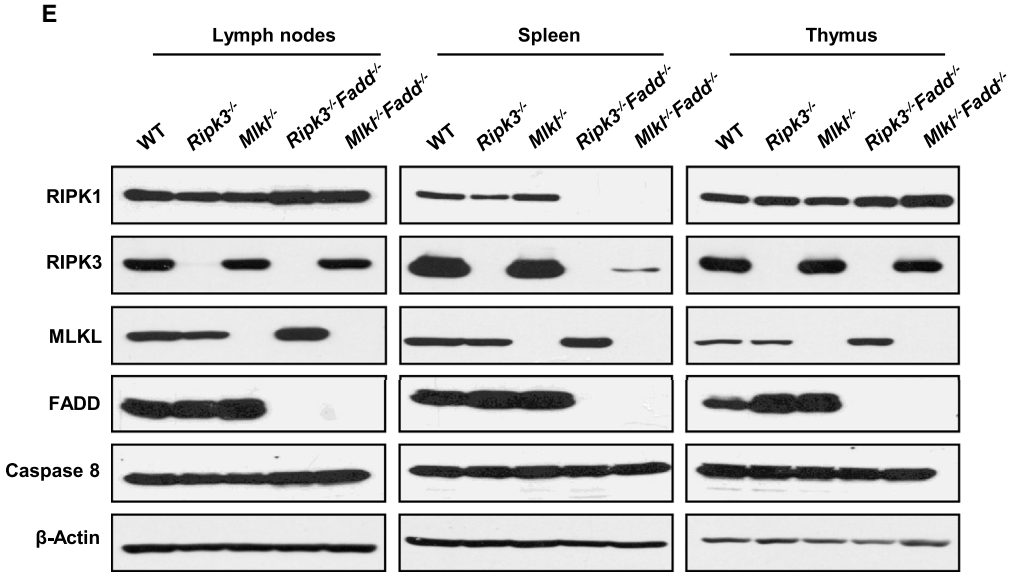

(legend on next page)

2011; Newton et al., 2014; Oberst et al., 2011). Meanwhile, this disease also occurred in mice and humans containing mutations in FAS or FASL (Wilson et al., 2009). It is notable that *Caspase-8*$^{-/-}$*Ripk3*$^{-/-}$*Ripk1*$^{-/-}$ mice that are backcrossed to C57BL/6 mice background show milder lymphoproliferative disease compared to *Caspase-8*$^{-/-}$*Ripk3*$^{-/-}$ mice (Rickard et al., 2014; Dillon et al., 2014; Dowling et al., 2015), whereas the TKO mice generated without backcrossing display an opposite phenotype (Kaiser et al., 2014). These results indicate that the extent of the backcross of knockout mice may have to do with the phenotypes. Interestingly, genetic loss of both FASL and TRAIL in mice displays more severe disease than in FASL mutant mice (Sedger et al., 2010), which indicates that FAS may be one of the death receptors involving in progressive lymphoproliferative disease. Together, the precise contributions of cell death pathways in the pathogenesis of lymphoproliferative disease remain unclear.

Another important process closely related to necrosis is inflammatory response. Damage-associated molecular patterns (DAMPs) released from necrotic cells stimulate immune cells through ligation of pattern recognition receptors (PRRs) to secret pro-inflammatory cytokines such as interleukin-1β (IL-1β) and IL-18, which subsequently activate host immune defenses against various pathogens. The maturation of IL-1β and IL-18 is mediated by cytosolic NOD-like receptors (NLRs) and HIN domain-containing family member AIM2, which associate with other proteins to form large multimeric complex that is known as the inflammasome (Agostini et al., 2004; Davis et al., 2011; Schroder and Tschopp, 2010). The NLRP3 inflammasome, the most extensively studied one, consists of NLRP3, the apoptosis-associated speck-like protein containing a CARD (ASC) and pro-caspase-1. Processed by the NLRP3 inflammasome, active caspase-1 subsequently promotes the maturation of the pro-inflammatory cytokines IL-1β and IL-18 (Fernandes-Alnemri et al., 2007; Latz et al., 2013; Schroder et al., 2012).

In *Caspase-8*-deficient bone-marrow-derived dendritic cells (BMDCs), the NLRP3 inflammasome can be activated by lipopolysaccharide (LPS) treatment alone in a RIPK3-dependent manner, which is consistent with the results from cells deficient in *XIAP*, *cIAP1*, and *cIAP2*. Similarly, treatment of bone-marrow-derived macrophages (BMDMs) or BMDCs with Smac mimetics leads to the NLRP3 inflammasome activation, which requires RIPK3 (Kang et al., 2013; Silke et al., 2015; Vince et al., 2012). These results indicate that cIAP or caspase-8 inhibits RIPK3 mediated the NLRP3 inflammasome activation. Nevertheless, recent studies show that *Fadd*$^{-/-}$*Ripk3*$^{-/-}$ and *Caspase-8*$^{-/-}$*Ripk3*$^{-/-}$ BMDMs are unable to activate the NLRP3 inflammasome upon stimulation while activation in *Ripk3*$^{-/-}$ BMDMs is normal. This result suggests that caspase-8 or FADD, instead of RIPK3, may play an important role in the NLRP3 inflammasome activation (Gurung et al., 2014; Silke et al., 2015). These seemingly contradictory results interest us in investigating the NLRP3 activation in MLKL and FADD double-knockout background.

In this study, we demonstrate that *Mlkl* deletion rescued embryonic lethality caused by *Fadd* deficiency. *Mlkl*$^{-/-}$*Fadd*$^{-/-}$ mice survived to adulthood but displayed severer lymphoproliferative disease compared to the *Ripk3*$^{-/-}$ *Fadd*$^{-/-}$ mice. Furthermore, we found that the NLRP3 inflammasome activation was inhibited in *Mlkl*$^{-/-}$*Fadd*$^{-/-}$ BMDMs and BMDCs when challenged with LPS or poly(I:C). Thus, our study revealed indispensable roles of MLKL in mediating embryonic lethality of *Fadd*-deficient mice and suppressing progressive lymphoproliferative disease, more importantly, the potential function of MLKL and FADD in regulating inflammasome activation.

RESULTS

Embryonic Lethality Caused by *Fadd* Deficiency Is Rescued by *Mlkl* Deletion

Ablation of *Fadd* in mice causes embryonic death in mice between E10.5 and E11.5, which is probably due to the massive necrosis (Figure 1A). To evaluate the in vivo function of MLKL in embryonic development, we performed targeted disruption of *Mlkl* by CRISPR/Cas9 gene mutation system and crossed the *Mlkl* knockout alleles into *Fadd* knockout mice (Figures S1A and S1B). As expected, *Mlkl* deletion rescued embryonic lethality caused by *Fadd* deficiency. The resulting *Mlkl*$^{-/-}$*Fadd*$^{-/-}$ mice were viable and fertile, and the newborns were weaned at expected frequencies (Figures 1B and 1C). *Mlkl*$^{-/-}$*Fadd*$^{-/-}$ mice were almost indistinguishable from their *Mlkl*$^{-/-}$ and wild-type littermates in physical appearance and growth (Figures 1B and 1D). The immunoblot results showed undetectable expression of MLKL and FADD in multiple organs of *Mlkl*$^{-/-}$*Fadd*$^{-/-}$ mice (Figures 1E and S1D). Previous studies have reported that the mice with specific deficiency of *Fadd* or *Caspase-8* in epithelial cells resulted in terminal ileitis or chronic intestinal inflammation, which was prevented by the co-deletion of *Ripk3* (Welz et al., 2011). Besides, keratinocyte-specific *Fadd* deficiency promoted RIPK3-dependent necroptosis and skin inflammation in mice (Bonnet et al., 2011). Consistent with these results, *Mlkl*$^{-/-}$*Fadd*$^{-/-}$ mice exhibited no sign of chronic inflammation in skin or intestine when observed for over 5 months (Figures 1B and S1C), suggesting that RIPK3-MLKL-mediated necroptosis in epithelial cells is likely to participate in the pro-inflammatory signaling pathways when caspase-8 or FADD is inhibited. In conclusion, these results demonstrate that MLKL functionally mediates the consequences of *Fadd* deficiency in vivo.

Mlkl$^{-/-}$*Fadd*$^{-/-}$ Mice Are Resistant to DR-Induced Apoptosis and Necroptosis

Cell death mostly initiates through the ligation of DRs and the signaling is relayed through a series of protein-protein

Figure 1. Embryonic Lethality in *Fadd* Deficiency Mice Is Rescued by *Mlkl* Deletion

(A) Photographs of embryos of the indicated genotypes at E11.5.

(B) Photographs of 12-week-old mice of the indicated genotypes.

(C) Predicted and observed frequencies of mice born following *Mlkl*$^{+/-}$*Fadd*$^{+/-}$ intercross. †Predicted embryonic lethal.

(D) Plot of weight of littermate wild-type, *Mlkl*$^{-/-}$, and *Mlkl*$^{-/-}$*Fadd*$^{-/-}$ mice.

(E) Immunoblot of RIPK1, RIPK3, MLKL, FADD, caspase-8, and β-actin of lymph nodes, spleen, and thymus from mice of the indicated genotypes.

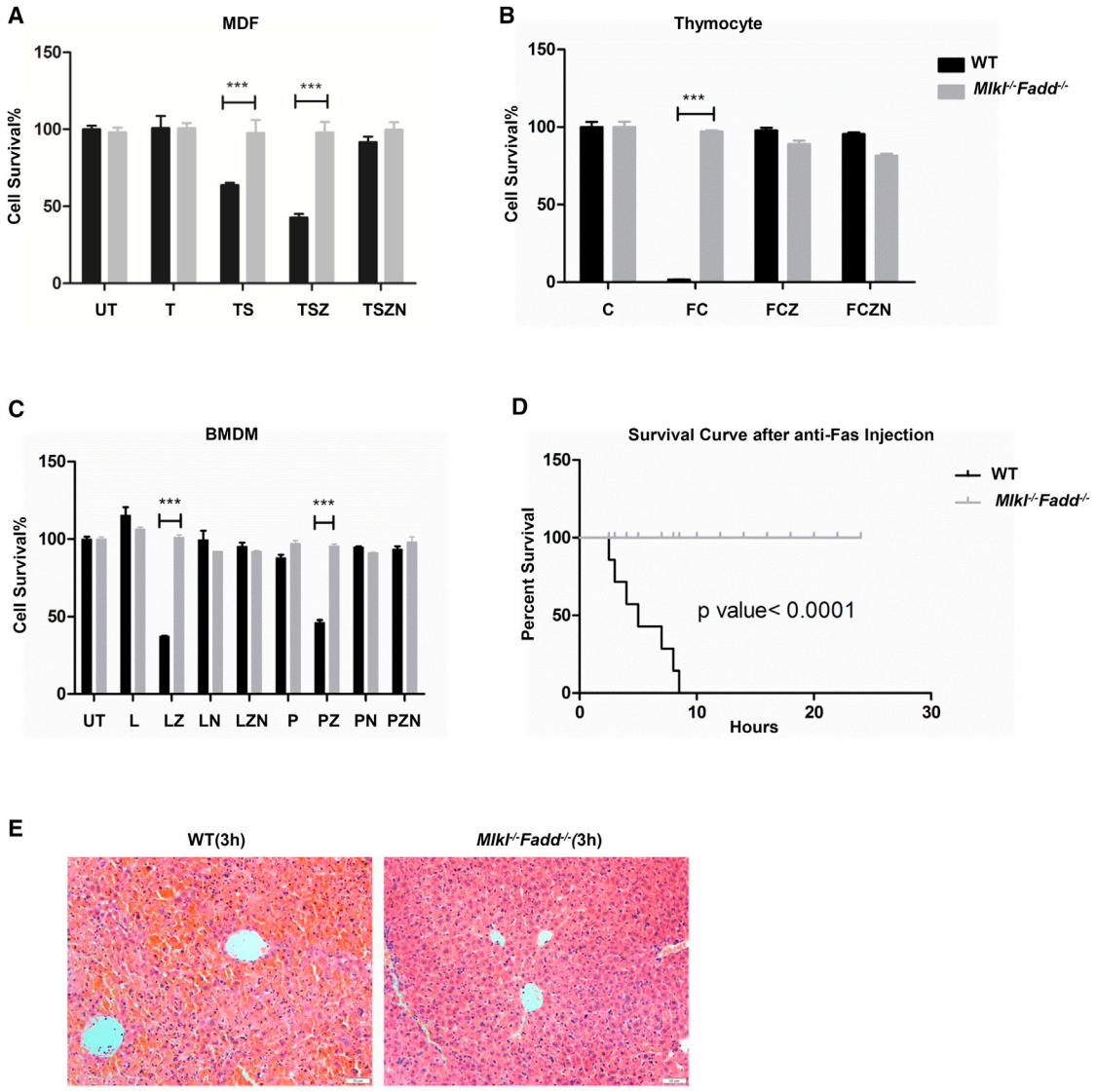

Figure 2. Sensitivities to DR-Induced Apoptosis and Necroptosis Both In Vitro and In Vivo

(A) Wild-type and littermate *Mlkl*$^{-/-}$*Fadd*$^{-/-}$ MDFs were treated with mouse TNF-α (30 ng/ml), TNF-α+Smac mimetic (100 nM), TNF-α+Smac mimetic+zVAD (20 μM), and TNF-α+ Smac mimetic+zVAD+Necrostatin1(30 μM), respectively.

(B) Thymuses from wild-type and littermate *Mlkl*$^{-/-}$*Fadd*$^{-/-}$ mice were milled and filtered into single cells. Thymocytes were treated with CHX (30 μg/ml), Fas ligand (100 ng/ml)+CHX, Fas ligand+CHX+zVAD (20 μM), and Fas ligand+CHX+zVAD+ Necrostatin1 (30 μM), respectively.

(C) Bone marrow from wild-type and littermate *Mlkl*$^{-/-}$*Fadd*$^{-/-}$ mice were induced by M-CSF (50 ng/ml) for 1 week. BMDMs from indicated genotypes were challenged with LPS (100 ng/ml), LPS+zVAD (20 μM), LPS+zVAD+Necrostatin1 (30 μM), Poly(I:C) (100 μg/ml), and Poly(I:C)+z VAD, Poly(I:C)+z VAD+Necrostatin-1, respectively.

(A–C) Cell viability was determined using the CellTiter-Glo kit. The data are represented as the mean ± SD of triplicate wells. ***p < 0.001(Student's t test). Abbreviations are as follows: UT, untreated; T, TNF-α; S, Smac mimetic; Z, zVAD; N, necrostatin. F, Fas ligand; C, CHX; L, LPS; P, Poly(I:C).

(D) Kaplan-Meier survival plot of 8-week-old wild-type (n = 7) and *Mlkl*$^{-/-}$*Fadd*$^{-/-}$ (n = 7) mice injected intraperitoneally with 12.5 μg of anti-Fas Jo-2 antibody.

(E) Histology of liver sections from wild-type (left panel) and *Mlkl*$^{-/-}$*Fadd*$^{-/-}$ (right panel) mice 3 hr after Jo-2 antibody injection. Scale bars, 50 μm.

interactions. To verify the disrupted functions of FADD and MLKL in *Mlkl*$^{-/-}$*Fadd*$^{-/-}$ mice, we tested several types of cells derived from wild-type (WT) and double-knockout (DKO) mice for their sensitivities to DR-induced cell death. As expected, WT mouse dermal fibroblasts (MDFs) had remarkable loss in response to the combined treatment with TNF and the cIAP inhibitor Smac mimetic. In the presence of caspase inhibitor zVAD-fmk, almost half of the WT MDFs underwent necroptosis which was inhibited by Necrostatin-1 (Figure 2A). Thymocytes were killed by treatment with anti-Fas antibodies (Figure 2B). In addition, BMDMs from WT mice were sensitive to LPS or Poly(I:C)-induced necroptosis (Figure 2C). In contrast to

WT cells, cells from *Mlkl*$^{-/-}$*Fadd*$^{-/-}$ mice were completely resistant to the extrinsic apoptosis and necroptosis triggered by the stimuli described above (Figures 2A–2C). Furthermore, *Mlkl*$^{-/-}$*Fadd*$^{-/-}$ mice were resistant to Fas-induced lethal hepatitis and survived for over 24 hr (Figure 2D) with normal liver architecture (Figure 2E). Together, these results show that FADD-dependent extrinsic apoptosis and MLKL-dependent necroptosis are blocked in *Mlkl*$^{-/-}$*Fadd*$^{-/-}$ cells, indicating that the functions of FADD and MLKL are eliminated in *Mlkl*$^{-/-}$*Fadd*$^{-/-}$ mice.

Mlkl$^{-/-}$*Fadd*$^{-/-}$ Mice Display More Severe Progressive Lymphoproliferative Disease Compared to *Ripk3*$^{-/-}$*Fadd*$^{-/-}$ Mice

In all settings where *Caspase-8* or *Fadd* deficiency has been rescued by elimination of *Ripk3* or the kinase activity of RIPK3, resulting viable mice exhibit lymphoid hyperplasia as they age (Dillon et al., 2012; Kaiser et al., 2011; Newton et al., 2014; Oberst et al., 2011). Similar to *Ripk3*$^{-/-}$*Fadd*$^{-/-}$ or *Ripk3*$^{-/-}$*Caspase-8*$^{-/-}$ mice, *Mlkl*$^{-/-}$*Fadd*$^{-/-}$ mice displayed swollen spleen and lymph nodes leading to a systematic lymphoproliferative disease over time but normal T cell population in thymus (Figures 3A, S2A, and S2C). Histology staining indicated excessive cell accumulation and abnormal structure in spleen and lymph nodes from *Mlkl*$^{-/-}$*Fadd*$^{-/-}$ mice (Figures 3B and S2B). Cells accumulated in spleen and lymph nodes were shown to be a population of B220^{+}CD3^{+} T lymphocytes (Figure 3C). Surprisingly, we observed that *Mlkl*$^{-/-}$*Fadd*$^{-/-}$ mice showed more severe lymphadenopathy and splenomegaly than *Ripk3*$^{-/-}$*Fadd*$^{-/-}$ mice did (Figures 3A, 3B, S2A, and S2B). Consistent with these phenotypes, a larger population of B220^{+}CD3^{+} T lymphocytes was accumulated in peripheral lymphoid organs (especially in lymph nodes) of *Mlkl*$^{-/-}$*Fadd*$^{-/-}$ mice in comparison with contemporary *Ripk3*$^{-/-}$*Fadd*$^{-/-}$ mice (Figure 3C). It seems that the remarkable distinction, comparing to *Ripk3*$^{-/-}$*Fadd*$^{-/-}$ mice, should owe to the praecox lymphoaccumulation (started around 9 weeks old, data not shown) and more rapid development of the disease in *Mlkl*$^{-/-}$*Fadd*$^{-/-}$ mice. Differences in organ sizes and B220^{+}CD3^{+} T lymphocytes percentage between two types of DKO mice became less significant over time (Figures 3A, 3C, and S2A). Aging mice to about 16 weeks old, we found enlarged parathymic lymph nodes emerged beside the thymus (it appeared earlier in *Mlkl*$^{-/-}$*Fadd*$^{-/-}$ mice than in *Ripk3*$^{-/-}$*Fadd*$^{-/-}$ mice), which were confirmed to be accumulations of B220^{+}CD3^{+} T lymphocytes similar to those shown in spleen and other lymph nodes (Figures 3A, S2A, and S2C). The faster accumulation of B220^{+}CD3^{+} T lymphocytes we observed in *Mlkl*$^{-/-}$*Fadd*$^{-/-}$ mice indicated a divergence between these two genotypes in cell proliferation. To test our hypothesis, we checked the cell proliferation in peripheral lymph organs using Ki67 staining. Compared with *Ripk3*$^{-/-}$*Fadd*$^{-/-}$ mice and WT controls, more Ki67 positive cells were detected in peripheral lymph organs of *Mlkl*$^{-/-}$*Fadd*$^{-/-}$ mice, indicating more active cell proliferation (Figure S2D). Thus, our data implicate that hyperproliferation of B220^{+}CD3^{+} T lymphocytes contributes to more severe lymphoproliferative disease in *Mlkl*$^{-/-}$*Fadd*$^{-/-}$ mice than in *Ripk3*$^{-/-}$*Fadd*$^{-/-}$ mice.

Mlkl$^{-/-}$*Fadd*$^{-/-}$ BMDMs Are Impaired in the NLRP3 Inflammasome Activation When Challenged with LPS or Poly(I:C)

Inflammasomes are large intracellular multiprotein complexes that play a central role in innate immunity. Recent studies have provided some evidence that FADD, RIPK3, and MLKL may be involved in regulating the NLRP3 inflammasome activation (Gurung et al., 2014; Kang et al., 2013, 2015; Lawlor et al., 2015; Silke et al., 2015; Vince et al., 2012). To investigate the function of these proteins in the NLRP3 inflammasome activation, we challenged *Ripk3*$^{-/-}$*Fadd*$^{-/-}$, *Mlkl*$^{-/-}$*Fadd*$^{-/-}$, *Ripk3*$^{-/-}$, and *Mlkl*$^{-/-}$ BMDMs with LPS for priming and subsequently stimulated them with ATP to activate the canonical NLRP3 inflammasome. In comparison with *Ripk3*$^{-/-}$ and *Mlkl*$^{-/-}$ BMDMs, caspase-1 processing was significantly reduced in *Ripk3*$^{-/-}$*Fadd*$^{-/-}$ and *Mlkl*$^{-/-}$*Fadd*$^{-/-}$ BMDMs (Figure 4A). Consistently, IL-1β secretion was significantly decreased in *Ripk3*$^{-/-}$*Fadd*$^{-/-}$ and *Mlkl*$^{-/-}$*Fadd*$^{-/-}$ BMDMs (Figure 4B). These BMDMs were also primed with poly(I:C) and treated with ATP for the inflammasome activation. Similar to the aforementioned results, *Mlkl*$^{-/-}$*Fadd*$^{-/-}$ BMDMs had little response to the treatment while the WT BMDMs had normal inflammasome activation (Figures 4C and 4D). Furthermore, the similar set of experiments was also performed in BMDCs. *Mlkl*$^{-/-}$*Fadd*$^{-/-}$ BMDCs were defective in NLRP3 inflammasome activation as well (Figures S4B and S4C). Previous studies have revealed that FADD and caspase-8 were apical mediators of canonical and noncanonical NLRP3 inflammasome activation (Kang et al., 2013; Silke et al., 2015; Vince et al., 2012; Gurung et al., 2014). To investigate the cause of the defect in DKO BMDMs, we examined the NLRP3 inflammasome activation in BMDMs derived from *LysM-cre*-mediated cell-specific *Fadd* deletion mice, and the deletion efficiency of FADD was tested by immunoblot (Figure S4A). The results showed that LPS or poly(I:C) primed BMDMs with low FADD expression had normal caspase-1 processing and IL-1β secretion upon stimulation as WT control (Figures 4E and 4F).

In conclusion, in contrast to the *Ripk3*$^{-/-}$, *Mlkl*$^{-/-}$and FADD insufficient BMDMs, *Ripk3*$^{-/-}$*Fadd*$^{-/-}$ and *Mlkl*$^{-/-}$*Fadd*$^{-/-}$ BMDMs or BMDCs have impaired canonical NLRP3 inflammasome activation when challenged with LPS or Poly(I:C). Our data suggest that MLKL is likely to function together with FADD to co-regulate the canonical NLRP3 inflammasome activation engaged through TLR3 or TLR4.

NLRP3 Inflammasome Activation Failure in *Mlkl*$^{-/-}$*Fadd*$^{-/-}$ BMDMs Is Due to Defects of ASC Speck Formation and NF-κB-Dependent NLRP3 Transcription

Formation of NLRP3 inflammasome requires the pyrin domain (PYD) of NLRP3 to recruit the adaptor protein ASC through PYD-PYD interaction. This interaction further facilitates the recruitment of pro-caspase-1 to assemble the inflammasome complex which is necessary for caspase-1 activation (Fernandes-Alnemri et al., 2007; Sutterwala et al., 2014).

To investigate whether the impaired inflammasome activation in *Mlkl*$^{-/-}$*Fadd*$^{-/-}$or *Ripk3*$^{-/-}$*Fadd*$^{-/-}$ BMDMs was due to a defect in the complex formation, we analyzed the ASC polymerization after LPS stimulation in *Mlkl*$^{-/-}$*Fadd*$^{-/-}$, *Ripk3*$^{-/-}$*Fadd*$^{-/-}$

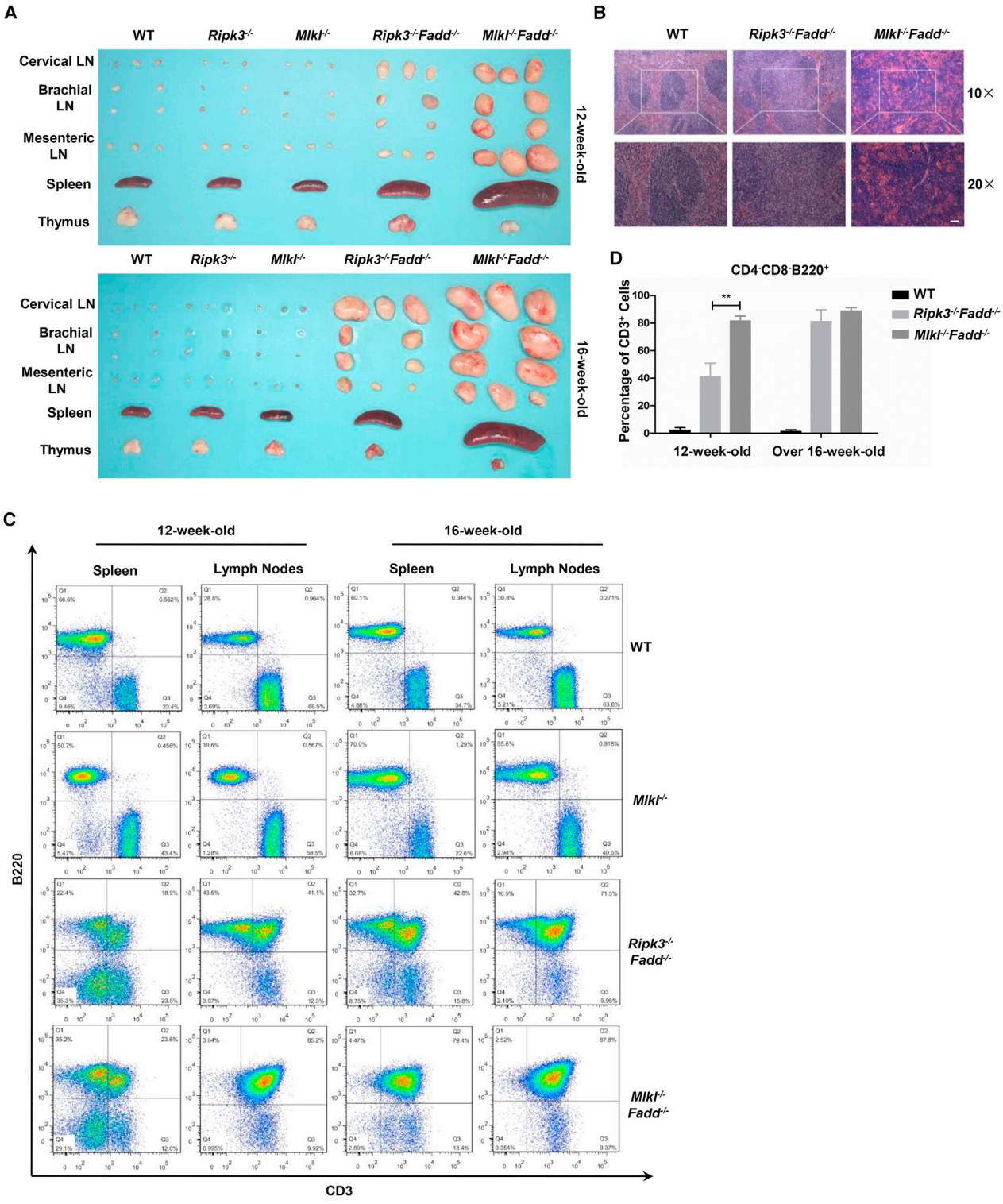

Figure 3. *Mlkl*$^{-/-}$*Fadd*$^{-/-}$ Mice Display More Severe Systemic Lymphoproliferative Disease Than *Ripk3*$^{-/-}$*Fadd*$^{-/-}$ Mice

(A) Lymph nodes, spleens, and thymus removed from 12- and 16-week-old mice of indicated genotypes.

(B) H&E-stained sections of fixed spleen from mice of indicated genotypes. Scale bars, 50 μm

(C) Percentage of B220^{+}CD3^{+} cells from spleen and lymph nodes in 12- mice or 16-week-old mice of the indicated genotypes.

(D) Percentage of CD3^{+} cells in CD4^{-}CD8^{-}B220^{+} populations from lymph nodes of mice with indicated genotypes and ages. Error bars, SD for three wild-type, three *Ripk3*$^{-/-}$*Fadd*$^{-/-}$ and three *Mlkl*$^{-/-}$*Fadd*$^{-/-}$ mice.

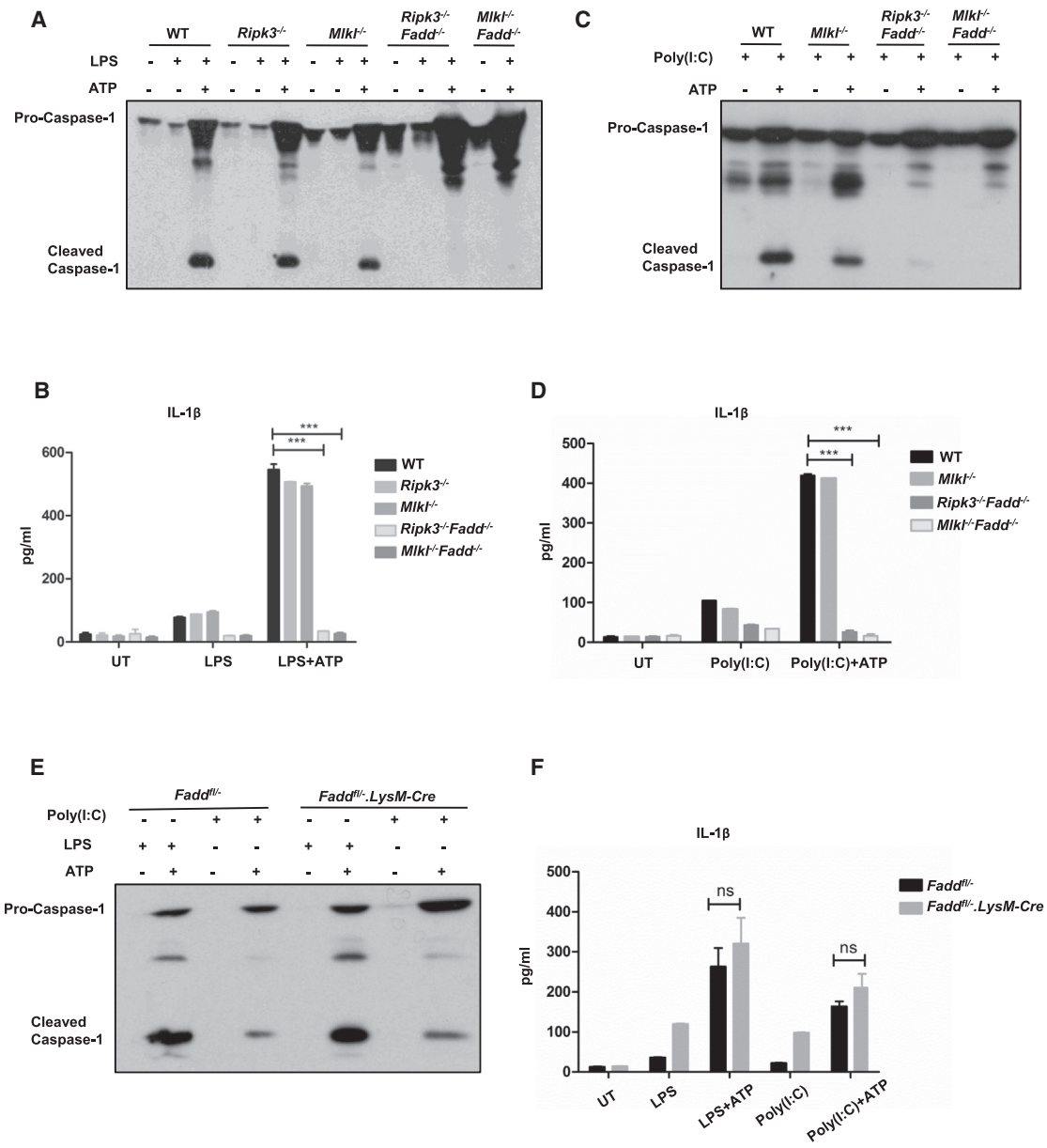

Figure 4. Activation of Canonical NLRP3 Inflammasome in BMDMs

(A and C) Wild-type, *Ripk3*$^{-/-}$, *Mlkl*$^{-/-}$, *Ripk3*$^{-/-}$*Fadd*$^{-/-}$, and *Mlkl*$^{-/-}$*Fadd*$^{-/-}$ BMDMs were primed with (A) 20 ng/ml LPS or (C) 100 μg/ml Poly(I:C) for 5 hr prior to 30-min treatment of 5 mM ATP. Supernatants were analyzed by immunoblot for caspase-1 activation.

(B and D) Wild-type, *Ripk3*$^{-/-}$, *Mlkl*$^{-/-}$, *Ripk3*$^{-/-}$*Fadd*$^{-/-}$, and *Mlkl*$^{-/-}$*Fadd*$^{-/-}$ BMDMs were stimulated with (B) 20 ng/ml LPS or (D) 100 μg/ml Poly(I:C) for 12 hr prior to 15-min treatment of 5 mM ATP. Supernatants were analyzed by ELISA for IL-1β secretion.

(E) Wild-type and FADD insufficient BMDMs were primed with 20 ng/ml LPS or (C) 100 μg/ml Poly(I:C) for 5 hr prior to 30-min treatment of 5 mM ATP. Supernatants were analyzed by immunoblot for caspase-1 activation and (F) were analyzed by ELISA for IL-1β secretion. ***$p < 0.001$ (Student's t test). n.s., not significant.

BMDMs, and controls. As expected, in contrast to controls, *Mlkl*$^{-/-}$*Fadd*$^{-/-}$ and *Ripk3*$^{-/-}$*Fadd*$^{-/-}$ BMDMs had significantly reduced ASC polymerization in both the pellet and the supernatant of cell lysates (Figure 5A). The same defects were shown in *Mlkl*$^{-/-}$*Fadd*$^{-/-}$ and *Ripk3*$^{-/-}$*Fadd*$^{-/-}$ BMDCs (Figure S4D). In line with the results above, significantly fewer ASC specks formed in *Mlkl*$^{-/-}$*Fadd*$^{-/-}$ BMDMs than in WT BMDMs (Figures 5B and 5C), suggesting that MLKL and FADD may mediate the NLRP3 inflammasome activation through regulating ASC speck formation.

As the key component of the inflammasome complex, NLRP3 can be upregulated by the priming signal. Thus, we examined both NLRP3 protein level and mRNA level by immunoblot and qRT-PCR, respectively. In *Mlkl*$^{-/-}$*Fadd*$^{-/-}$ and *Ripk3*$^{-/-}$*Fadd*$^{-/-}$

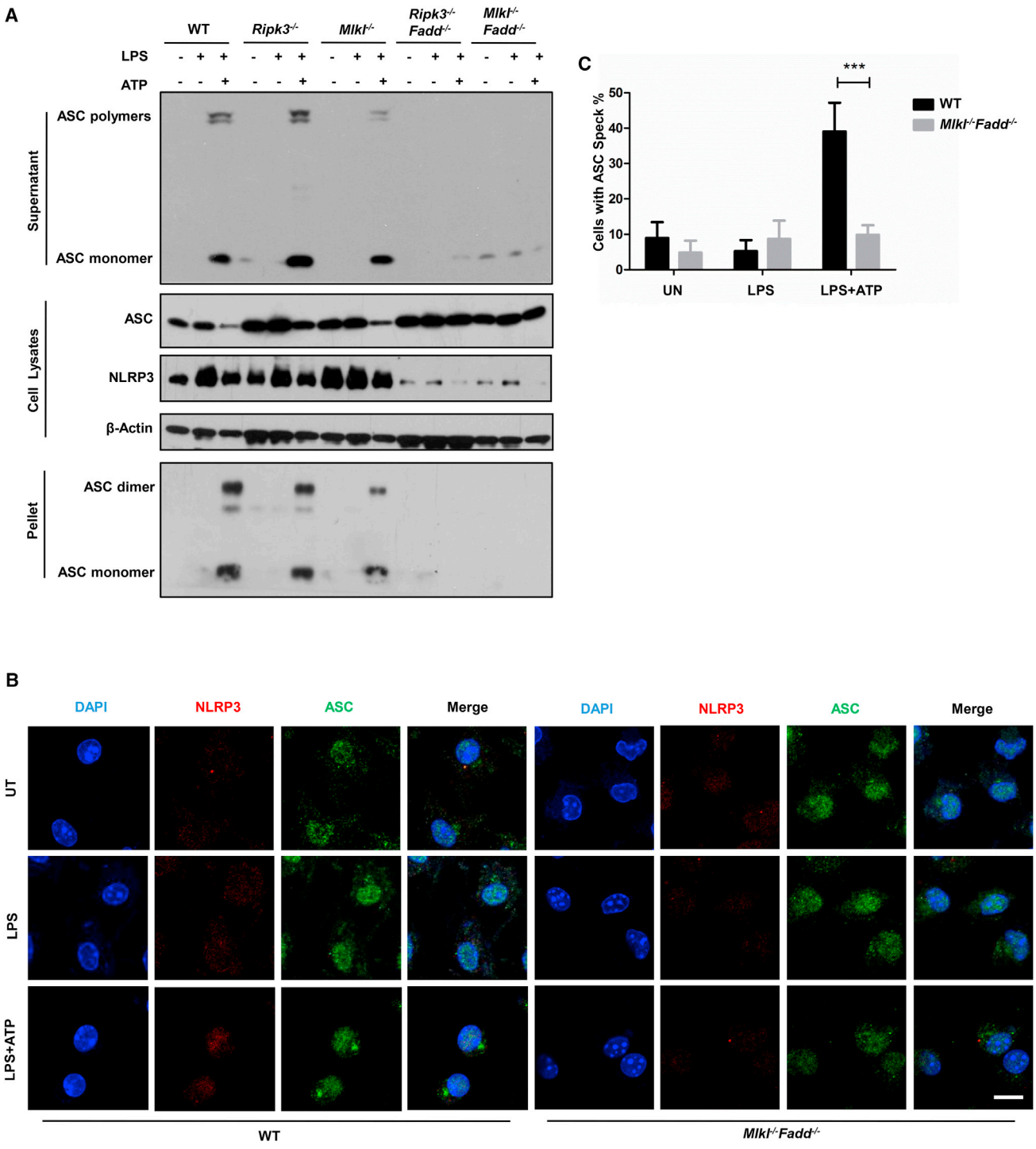

Figure 5. ASC Polymerization in BMDMs upon LPS Stimulation

(A) Wild-type, *Ripk3*$^{-/-}$, *Mlkl*$^{-/-}$, *Ripk3*$^{-/-}$*Fadd*$^{-/-}$, and *Mlkl*$^{-/-}$*Fadd*$^{-/-}$ BMDMs or for 5 hr prior to 30-min treatment of 5 mM ATP. Supernatants and cell pellets were analyzed by immunoblot for ASC polymerization. Cell lysates were analyzed by immunoblot for the expression of ASC and NLRP3.

(B) Immunofluorescence microscopy of LPS-primed wild-type *Mlkl*$^{-/-}$*Fadd*$^{-/-}$ BMDMs without or with 5 mM ATP treatment, top (untreated), middle (LPS primed), and bottom (ATP stimulation after LPS priming). Cells were fixed and immunostained for ASC (green) and NLRP3 (red). DAPI (blue) was used for nuclear staining. Scale bars, 5 μm.

(C) Quantification of results from Figure 4B. Total cells and cells with an ASC polymer (speck) were counted, and the percentages of cells with ASC polymer were calculated. The data are represented as the mean ± SD of five microscopic fields per group.

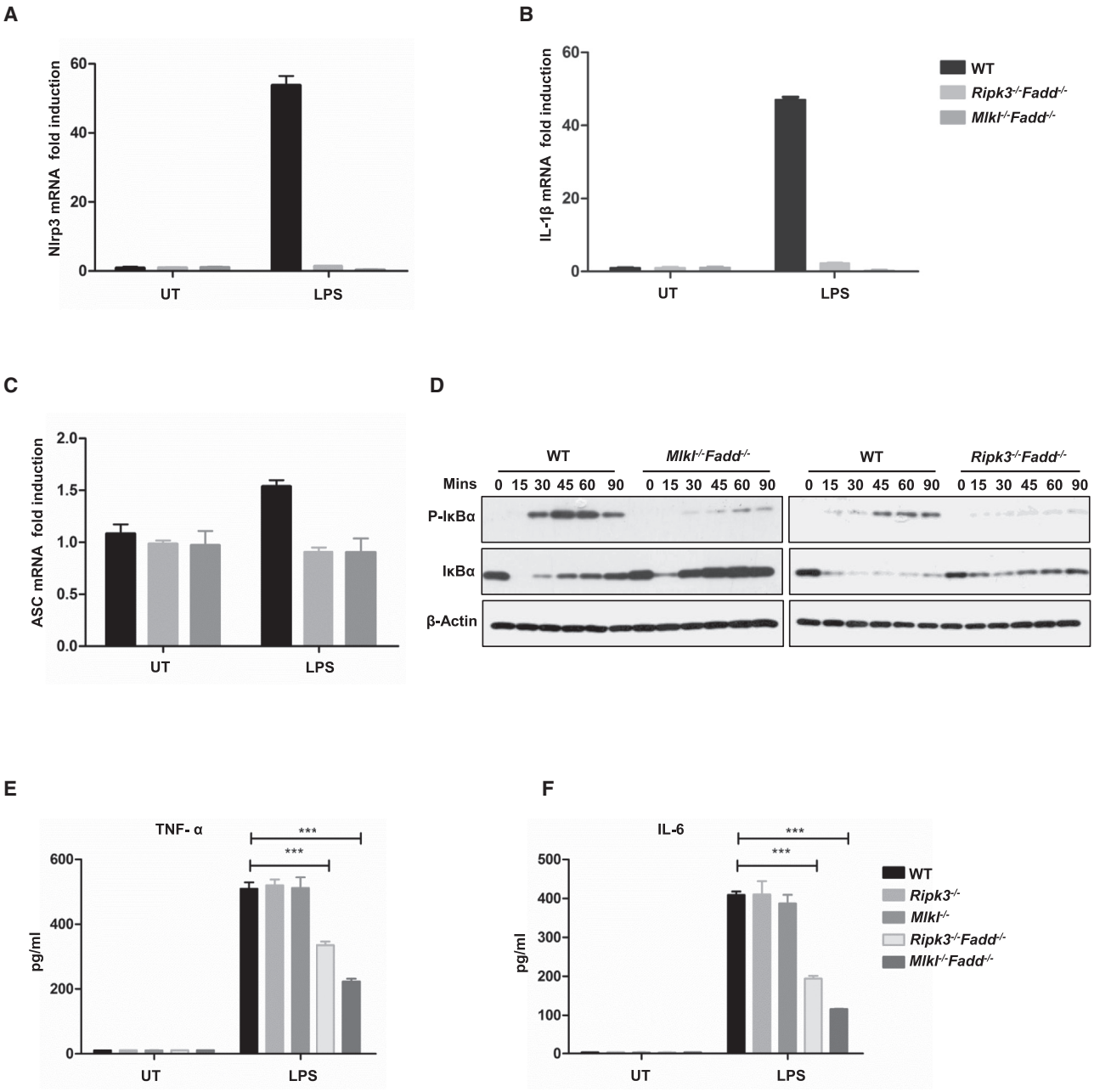

Figure 6. NF-κB Activation in BMDMs upon LPS Stimulation

(A–C) Wild-type, *Ripk3*$^{-/-}$*Fadd*$^{-/-}$, and *Mlkl*$^{-/-}$*Fadd*$^{-/-}$ BMDMs were treated with 20 ng/ml LPS for 6 hr, and mRNA levels of NLRP3 (A), IL-1β (B), and ASC (C) were determined by qPCR.

(D)Wild-type and *Mlkl*$^{-/-}$*Fadd*$^{-/-}$ BMDMs were treated with 100 ng/ml LPS for 15, 30, 60, and 90 min, respectively. The expression of indicated the proteins were detected by western blot.

(E and F) Wild-type, *Ripk3*$^{-/-}$, *Mlkl*$^{-/-}$, *Ripk3*$^{-/-}$*Fadd*$^{-/-}$, and *Mlkl*$^{-/-}$*Fadd*$^{-/-}$ BMDMs were treated with 20 ng/ml LPS for 12 hr. Supernatants were collected for the detections of TNF-α and IL-6 by ELISA.

BMDMs treated with LPS, NLRP3 can hardly respond to the priming signal compared with WT control while ASC had normal transcription and expression levels in all BMDMs (Figures 5A, 6A, and 6C). Besides, pro-IL1β, the substrate of the activated inflammasome, was unable to be upregulated in *Mlkl*$^{-/-}$*Fadd*$^{-/-}$ and *Ripk3*$^{-/-}$*Fadd*$^{-/-}$ BMDMs either (Figure 6B).

Given that *NLRP3* and *pro-IL-1β*are transcriptionally regulated by NF-κB, we therefore examined NF-κB signals following LPS stimulation in *Mlkl*$^{-/-}$*Fadd*$^{-/-}$ and wild-type BMDMs by

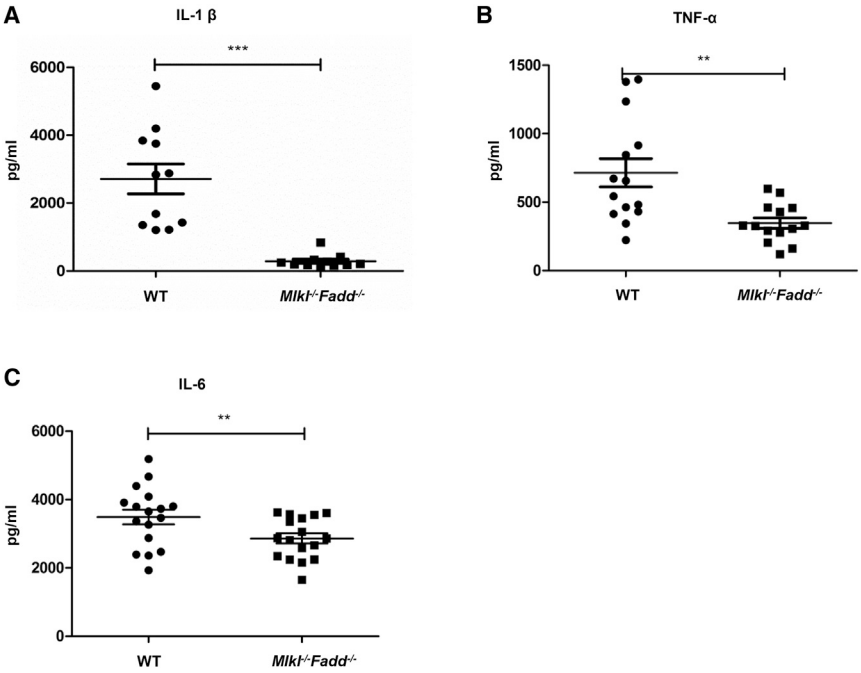

Figure 7. Decreasing Cytokine Secretion in *Mlkl*$^{-/-}$*Fadd*$^{-/-}$ Mice

(A–C) Wild-type and *Mlkl*$^{-/-}$*Fadd*$^{-/-}$ mice were challenged with LPS (i.p., 54 mg/kg), and the productions of serum IL-1β (A), TNF-α (B), and IL-6 (C) were detected by ELISA 12 hr later. Each dot represents one mouse.

immunoblots (Bauernfeind et al., 2009; Schroder et al., 2012; Sutterwala et al., 2014). We found that NF-κB activation was significantly decreased associated with less phosphorylation and degradation of IκB in both *Mlkl*$^{-/-}$*Fadd*$^{-/-}$ and *Ripk3*$^{-/-}$*Fadd*$^{-/-}$ BMDMs than in WT BMDMs (Figure 6D). Furthermore, we examined the secretion levels of TNF-α and IL-6, which are the target genes of NF-κB. It was shown that *Mlkl*$^{-/-}$*Fadd*$^{-/-}$ BMDMs had notable reduction of TNF-α and IL-6 levels in comparison to WT controls (Figures 6E and 6F).

In summary, our findings suggest that the NLRP3 inflammasome formation is insensitive to LPS/ATP stimulation in *Mlkl*$^{-/-}$*Fadd*$^{-/-}$ and *Ripk3*$^{-/-}$*Fadd*$^{-/-}$ BMDMs. This is likely due to the defects in NF-κB-dependent *Nlrp3* and *pro-IL-1β* transcriptions. Consequently, the lack of NLRP3 and pro-IL-1β expression renders the *Mlkl*$^{-/-}$*Fadd*$^{-/-}$ and *Ripk3*$^{-/-}$*Fadd*$^{-/-}$ BMDMs incapable of forming ASC speck and recruiting other components to assemble the NLRP3 inflammasome complex, which results in the failure of caspase-1 processing and mature IL-1β secretion.

DISCUSSION

The findings of our study provide genetic evidence that MLKL mediates the embryonic lethality of *Fadd* deficiency in vivo. Combined with previous studies (Dillon et al., 2012; Kaiser et al., 2011; Oberst et al., 2011; Varfolomeev et al., 1998; Yeh et al., 1998), we speculate that, during the embryonic development, RIPK3-MLKL-mediated necroptotic signaling is tightly regulated by the caspase-8-FADD-cFLIP complex although the function of MLKL in the condition of *Caspase-8* genetic ablation remains to be identified. Several studies have intimated that *Fadd* or *Caspase-8* deficiency induced RIPK3-dependent pathway may target the yolk sac vasculature and hematopoietic cells during embryogenesis. However, direct evidence showing that embryonic lethality of *Fadd*-deficient mice is caused by RIPK3-MLKL-mediating necroptosis must still be obtained.

Considering that the CRISPR/Cas9 system could introduce off-target effects in the *Mlkl* knockout mice, we confirmed the phenotypes using another *Mlkl* knockout mouse line that was generated by an independent single guide (sg)RNA (Figures S3A and S3B). The two independent lines of *Mlkl* knockout mice were individually crossed into the same line of *Fadd*-deficient mice, and the two lineages displayed equivalent properties, excluding the possibility that off-target effects contributed to the phenotypes of *Mlkl*$^{-/-}$*Fadd*$^{-/-}$ mice (Figure S3C).

Previous studies have demonstrated that FASL-FAS signaling kills unwanted cells through FADD/caspase-8-mediated apoptosis during the development of lymphocytes. Conditional deletion of *Fadd* or *Caspase-8* in T cell results in proliferation defects in response to activation signals (Zhang et al., 1998; Kabra et al., 2001; Salmena et al., 2003; Ch'en et al., 2008), while combined deletion of either *Ripk3* or *Mlkl* and *Fadd* in an intact germline leads to accumulation of abnormal CD3^{+}B220^{+} T cells. Given that MLKL works downstream of RIPK3, we hypothesize that the lack of MLKL may block other possible undefined cell signaling pathways independent of RIPK3, resulting in the praecox accumulation of CD3^{+}B220^{+} T cells in spleen and lymph nodes in *Mlkl*$^{-/-}$*Fadd*$^{-/-}$ mice. Another possibility is that more cell proliferation occurring in *Mlkl*$^{-/-}$*Fadd*$^{-/-}$ mice leads to severer lymphoproliferative disease. However, the precise mechanisms behind the interesting phenotypes remain to be explored.

A high dose of LPS results in endotoxemia in mice and subsequently leads to the massive systemic release of pro-inflammatory cytokines. When we challenged *Mlkl*$^{-/-}$*Fadd*$^{-/-}$ mice with LPS to assess the capacity of initiating innate immunity, we observed a dramatic reduction of cytokine release in *Mlkl*$^{-/-}$*Fadd*$^{-/-}$ mice (Figures 7A–7C). We speculate that the reduced cytokine secretion was due to impaired activation of the NLRP3 inflammasome and NF-κB signaling as shown in the previous investigations in *Ripk3*$^{-/-}$*Fadd*$^{-/-}$ mice and *Ripk3*$^{-/-}$*Casp8*$^{-/-}$ mice (Gurung et al., 2014; Kang et al., 2013). The defects in both DKO mice raise an important issue about how the NF-κB signaling in DKO BMDMs is regulated. Although conditional deletion of *Fadd* in BMDMs have negligible effects on the activation of inflammasome upon the

stimulation of LPS or Poly(I:C) as *Mlkl*$^{-/-}$ or *Rip3*$^{-/-}$ BMDMs (Figures 4E and 4F), it remains likely that FADD alone determines the NLRP3 inflammasome activation due to its incomplete deletion (Figure S4A). Thus, we hypothesized that RIPK3/MLKL and FADD/caspase-8 may co-regulate a target or targets that mediate NF-κB signaling upon LPS or Poly(I:C) stimulation. Nevertheless, the functions of these proteins in regulating the targets need to be clarified by sophisticated biochemical studies, and their functions in activating non-canonical NLRP3 inflammasome and other types of inflammasomes should be further investigated.

The findings that FADD restricted MLKL-dependent pathway during embryonic development and in maintaining the homeostasis of T cell suggest the importance of the interplay between FADD-dependent apoptosis and MLKL-dependent necroptosis. More importantly, the key components of the two cell death pathways may function as regulators in other situations as we have observed in stimulating BMDMs or BMDCs. In this light, it is noteworthy that our findings here point out MLKL and FADD, which are multifunctional in regulating cell death and innate immune response, have broad implications for the related investigations as well as approaches to therapies of cancer and immune disorders.

EXPERIMENTAL PROCEDURES

Reagents

LPS, ATP, and PolyI:C were obtained from Sigma. TNF-α and z-VAD were from R&D Systems and Calbiochem, respectively. Necrostatin-1 was purchased from Enzo Life Sciences. The following antibodies were used for western blotting and immunofluorescence experiments: RIPK1 (BD Biosciences), RIPK3 (Prosci), IκBα and p- IκBα (Cell Signaling Technology), ASC (Santa Cruz Biotechnology), IL-1β (Santa Cruz), mouse caspase-1 (AdipoGen), NLRP3 (R&D). MLKL antibody was a gift from Dr. Jiahuai Han (Xiamen University). FADD antibody was from Dr. Jianke Zhang (Thomas Jefferson University). Mouse TNF-α, IL-6, and IL-1β ELISA Kits were from MultiSciences. Cell viability was determined by measuring ATP levels using the Cell Titer-Glo kit (Promega).

Mice

Mice were housed in a specific pathogen-free (SPF) facility. *Ripk3* knockout mice were provided by Dr. Xiaodong Wang (NIBS, Beijing, China), and *Fadd*$^{-/-}$*Tg* mice were provided by Dr. Jianke Zhang (Thomas Jefferson University). *Mlkl* knockout mice were generated by CRISPR-Cas9 mutation system (Bioray Laboratories). A 301-bp deletion in the *Mlkl* gene was introduced in the *Mlkl* locus, and genotyping results of mice are presented in Figures S1A and S1B. Additional information is provided upon request. Animal experiments were conducted in accordance with the guidelines of the Institutional Animal Care and Use Committee of the Institute for Nutritional Sciences, Shanghai Institutes for Biological Sciences, Chinese Academy of Sciences (CAS).

Cell Survival Assay

Cell survival was determined using the CellTiter-Glo Luminescent Cell Viability Assay kit, and the luminescence was recorded with a microplate luminometer (Thermo Scientific).

Isolation of Mouse BMDMs and Inflammasome Activation

Bone marrow cells were collected from mouse femurs and tibias and were cultured for 7 days in RPMI medium containing 10% fetal bovine serum (FBS), penicillin, streptomycin, and 50 ng/ml M-CSF. Medium was changed every 2 days. BMDMs were induced to differentiate in vitro from isolated bone marrow cells. For inflammasome assays, BMDMs were pretreated with LPS or Poly(I:C) for 5 hr before stimulated with ATP (5 mM) for 30 min. The media supernatant and cell lysates were collected for precipitation and immunoblot analysis.

ASC Oligomerization Detection

ASC pyroptosomes were detected as previously reported (Juliana et al., 2010). Macrophages were seeded in 6-well plates (2×10^6 cells per well) and treated with different stimuli. The cells were pelleted by centrifugation and resuspended in 0.5 ml of ice-cold buffer containing 20 mM HEPES-KOH (pH 7.5), 150 mM KCl, 1% Nonidet P-40, 0.1 mM PMSF, and a protease inhibitor mixture. Cell lysates were centrifuged at 5,000 × *g* for 10 min at 4°C, and pellets were washed twice with PBS before being resuspended in 500 μl of PBS. The pellets were crosslinked with fresh DSS (4 mM) for 30 min and pelleted by centrifugation at 5,000 × *g* for 10 min. Crosslinked pellets were resuspended in 30 μl of SDS sample buffer and subjected to western blot with the anti-mouse ASC antibodies.

Statistical Analysis

Data presented in this article are representative results of at least three independent experiments. The in vitro results were presented as the mean ± SD of triplicate wells. The statistical significance of data was evaluated by Student's t test in which $p < 0.01$ was considered significant and $p < 0.001$ was highly significant. The statistical calculations were performed with GraphPad Prism software.

SUPPLEMENTAL INFORMATION

Supplemental Information includes Supplemental Experimental Procedures and four figures and can be found with this article online at http://dx.doi.org/10.1016/j.celrep.2016.06.103.

AUTHOR CONTRIBUTIONS

X.Z. and Haibing Zhang designed the study and planned the experiments; X.Z., C.F., and Haiwei Zhang performed the experiments and analyzed data with assistance from Q.Z., Y.L., C.X., Q.X., X.W., and X.Y.; J.Z. provided reagents and edited the manuscript; X.Z. and Haibing Zhang wrote the paper with assistance from C.F. and Haiwei Zhang; Haibing Zhang conceived and supervised the project.

ACKNOWLEDGMENTS

We thank Dr. Xiaodong Wang (National Institute of Biological Sciences) for providing *RIPK3*$^{-/-}$ mice and Dr. Jiahuai Han (Xiamen University) for providing mouse MLKL antibody. We thank Dr. Yu Sun (UCLA) for editing the manuscript and helpful discussion. We also thank Animal Facility of Institute for Nutritional Sciences for mouse care. This work was supported by grants from the National Natural Science Foundation of China (31571426 and 81502548). Haibing Zhang was supported by Thousand Young Talents Program of the Chinese government.

Received: December 1, 2015
Revised: April 1, 2016
Accepted: June 23, 2016
Published: August 4, 2016

REFERENCES

Agostini, L., Martinon, F., Burns, K., McDermott, M.F., Hawkins, P.N., and Tschopp, J. (2004). NALP3 forms an IL-1beta-processing inflammasome with increased activity in Muckle-Wells autoinflammatory disorder. Immunity *20*, 319–325.

Bauernfeind, F.G., Horvath, G., Stutz, A., Alnemri, E.S., MacDonald, K., Speert, D., Fernandes-Alnemri, T., Wu, J., Monks, B.G., Fitzgerald, K.A., et al. (2009). Cutting edge: NF-kappaB activating pattern recognition and cytokine receptors license NLRP3 inflammasome activation by regulating NLRP3 expression. J. Immunol. *183*, 787–791.

Boldin, M.P., Goncharov, T.M., Goltsev, Y.V., and Wallach, D. (1996). Involvement of MACH, a novel MORT1/FADD-interacting protease, in Fas/APO-1- and TNF receptor-induced cell death. Cell *85*, 803–815.

Bonnet, M.C., Preukschat, D., Welz, P.S., van Loo, G., Ermolaeva, M.A., Bloch, W., Haase, I., and Pasparakis, M. (2011). The adaptor protein FADD protects epidermal keratinocytes from necroptosis in vivo and prevents skin inflammation. Immunity *35*, 572–582.

Cai, Z., Jitkaew, S., Zhao, J., Chiang, H.C., Choksi, S., Liu, J., Ward, Y., Wu, L.G., and Liu, Z.G. (2014). Plasma membrane translocation of trimerized MLKL protein is required for TNF-induced necroptosis. Nat. Cell Biol. *16*, 55–65.

Ch'en, I.L., Beisner, D.R., Degterev, A., Lynch, C., Yuan, J., Hoffmann, A., and Hedrick, S.M. (2008). Antigen-mediated T cell expansion regulated by parallel pathways of death. Proc. Natl. Acad. Sci. USA *105*, 17463–17468.

Chen, X., Li, W., Ren, J., Huang, D., He, W.T., Song, Y., Yang, C., Li, W., Zheng, X., Chen, P., and Han, J. (2014). Translocation of mixed lineage kinase domain-like protein to plasma membrane leads to necrotic cell death. Cell Res. *24*, 105–121.

Davis, B.K., Wen, H., and Ting, J.P.Y. (2011). The inflammasome NLRs in immunity, inflammation, and associated diseases. Annu. Rev. Immunol. *29*, 707–735.

Dillon, C.P., Oberst, A., Weinlich, R., Janke, L.J., Kang, T.B., Ben-Moshe, T., Mak, T.W., Wallach, D., and Green, D.R. (2012). Survival function of the FADD-CASPASE-8-cFLIP(L) complex. Cell Rep. *1*, 401–407.

Dillon, C.P., Weinlich, R., Rodriguez, D.A., Cripps, J.G., Quarato, G., Gurung, P., Verbist, K.C., Brewer, T.L., Llambi, F., Gong, Y.N., et al. (2014). RIPK1 blocks early postnatal lethality mediated by caspase-8 and RIPK3. Cell *157*, 1189–1202.

Dondelinger, Y., Declercq, W., Montessuit, S., Roelandt, R., Goncalves, A., Bruggeman, I., Hulpiau, P., Weber, K., Sehon, C.A., Marquis, R.W., et al. (2014). MLKL compromises plasma membrane integrity by binding to phosphatidylinositol phosphates. Cell Rep. *7*, 971–981.

Dowling, J.P., Nair, A., and Zhang, J. (2015). A novel function of RIP1 in postnatal development and immune homeostasis by protecting against RIP3-dependent necroptosis and FADD-mediated apoptosis. Front. Cell Dev. Biol. *3*, 12.

Fernandes-Alnemri, T., Wu, J., Yu, J.W., Datta, P., Miller, B., Jankowski, W., Rosenberg, S., Zhang, J., and Alnemri, E.S. (2007). The pyroptosome: a supramolecular assembly of ASC dimers mediating inflammatory cell death via caspase-1 activation. Cell Death Differ. *14*, 1590–1604.

Gurung, P., Anand, P.K., Malireddi, R.K.S., Vande Walle, L., Van Opdenbosch, N., Dillon, C.P., Weinlich, R., Green, D.R., Lamkanfi, M., and Kanneganti, T.D. (2014). FADD and caspase-8 mediate priming and activation of the canonical and noncanonical Nlrp3 inflammasomes. J. Immunol. *192*, 1835–1846.

Juliana, C., Fernandes-Alnemri, T., Wu, J., Datta, P., Solorzano, L., Yu, J.W., Meng, R., Quong, A.A., Latz, E., Scott, C.P., and Alnemri, E.S. (2010). Anti-inflammatory compounds parthenolide and Bay 11-7082 are direct inhibitors of the inflammasome. J. Biol. Chem. *285*, 9792–9802.

Kabra, N.H., Kang, C., Hsing, L.C., Zhang, J., and Winoto, A. (2001). T cell-specific FADD-deficient mice: FADD is required for early T cell development. Proc. Natl. Acad. Sci. USA *98*, 6307–6312.

Kaiser, W.J., Upton, J.W., Long, A.B., Livingston-Rosanoff, D., Daley-Bauer, L.P., Hakem, R., Caspary, T., and Mocarski, E.S. (2011). RIP3 mediates the embryonic lethality of caspase-8-deficient mice. Nature *471*, 368–372.

Kaiser, W.J., Daley-Bauer, L.P., Thapa, R.J., Mandal, P., Berger, S.B., Huang, C., Sundararajan, A., Guo, H., Roback, L., Speck, S.H., et al. (2014). RIP1 suppresses innate immune necrotic as well as apoptotic cell death during mammalian parturition. Proc. Natl. Acad. Sci. USA *111*, 7753–7758.

Kang, T.B., Ben-Moshe, T., Varfolomeev, E.E., Pewzner-Jung, Y., Yogev, N., Jurewicz, A., Waisman, A., Brenner, O., Haffner, R., Gustafsson, E., et al. (2004). Caspase-8 serves both apoptotic and nonapoptotic roles. J. Immunol. *173*, 2976–2984.

Kang, T.B., Oh, G.S., Scandella, E., Bolinger, B., Ludewig, B., Kovalenko, A., and Wallach, D. (2008). Mutation of a self-processing site in caspase-8 compromises its apoptotic but not its nonapoptotic functions in bacterial artificial chromosome-transgenic mice. J. Immunol. *181*, 2522–2532.

Kang, T.B., Yang, S.H., Toth, B., Kovalenko, A., and Wallach, D. (2013). Caspase-8 blocks kinase RIPK3-mediated activation of the NLRP3 inflammasome. Immunity *38*, 27–40.

Kang, S., Fernandes-Alnemri, T., Rogers, C., Mayes, L., Wang, Y., Dillon, C., Roback, L., Kaiser, W., Oberst, A., Sagara, J., et al. (2015). Caspase-8 scaffolding function and MLKL regulate NLRP3 inflammasome activation downstream of TLR3. Nat. Commun. *6*, 7515.

Kelliher, M.A., Grimm, S., Ishida, Y., Kuo, F., Stanger, B.Z., and Leder, P. (1998). The death domain kinase RIP mediates the TNF-induced NF-kappaB signal. Immunity *8*, 297–303.

Latz, E., Xiao, T.S., and Stutz, A. (2013). Activation and regulation of the inflammasomes. Nat. Rev. Immunol. *13*, 397–411.

Lawlor, K.E., Khan, N., Mildenhall, A., Gerlic, M., Croker, B.A., D'Cruz, A.A., Hall, C., Kaur Spall, S., Anderton, H., Masters, S.L., et al. (2015). RIPK3 promotes cell death and NLRP3 inflammasome activation in the absence of MLKL. Nat. Commun. *6*, 6282.

Li, J., McQuade, T., Siemer, A.B., Napetschnig, J., Moriwaki, K., Hsiao, Y.S., Damko, E., Moquin, D., Walz, T., McDermott, A., et al. (2012). The RIP1/RIP3 necrosome forms a functional amyloid signaling complex required for programmed necrosis. Cell *150*, 339–350.

Muzio, M., Chinnaiyan, A.M., Kischkel, F.C., O'Rourke, K., Shevchenko, A., Ni, J., Scaffidi, C., Bretz, J.D., Zhang, M., Gentz, R., et al. (1996). FLICE, a novel FADD-homologous ICE/CED-3-like protease, is recruited to the CD95 (Fas/APO-1) death–inducing signaling complex. Cell *85*, 817–827.

Nagata, S. (1997). Apoptosis by death factor. Cell *88*, 355–365.

Newton, K., Dugger, D.L., Wickliffe, K.E., Kapoor, N., de Almagro, M.C., Vucic, D., Komuves, L., Ferrando, R.E., French, D.M., Webster, J., et al. (2014). Activity of protein kinase RIPK3 determines whether cells die by necroptosis or apoptosis. Science *343*, 1357–1360.

Oberst, A., Dillon, C.P., Weinlich, R., McCormick, L.L., Fitzgerald, P., Pop, C., Hakem, R., Salvesen, G.S., and Green, D.R. (2011). Catalytic activity of the caspase-8-FLIP(L) complex inhibits RIPK3-dependent necrosis. Nature *471*, 363–367.

Orozco, S., Yatim, N., Werner, M.R., Tran, H., Gunja, S.Y., Tait, S.W., Albert, M.L., Green, D.R., and Oberst, A. (2014). RIPK1 both positively and negatively regulates RIPK3 oligomerization and necroptosis. Cell Death Differ. *21*, 1511–1521.

Rickard, J.A., O'Donnell, J.A., Evans, J.M., Lalaoui, N., Poh, A.R., Rogers, T., Vince, J.E., Lawlor, K.E., Ninnis, R.L., Anderton, H., et al. (2014). RIPK1 regulates RIPK3-MLKL-driven systemic inflammation and emergency hematopoiesis. Cell *157*, 1175–1188.

Sakamaki, K., Inoue, T., Asano, M., Sudo, K., Kazama, H., Sakagami, J., Sakata, S., Ozaki, M., Nakamura, S., Toyokuni, S., et al. (2002). Ex vivo whole-embryo culture of caspase-8-deficient embryos normalize their aberrant phenotypes in the developing neural tube and heart. Cell Death Differ. *9*, 1196–1206.

Salmena, L., Lemmers, B., Hakem, A., Matysiak-Zablocki, E., Murakami, K., Au, P.Y.B., Berry, D.M., Tamblyn, L., Shehabeldin, A., Migon, E., et al. (2003). Essential role for caspase 8 in T-cell homeostasis and T-cell-mediated immunity. Genes Dev. *17*, 883–895.

Schroder, K., and Tschopp, J. (2010). The inflammasomes. Cell *140*, 821–832.

Schroder, K., Sagulenko, V., Zamoshnikova, A., Richards, A.A., Cridland, J.A., Irvine, K.M., Stacey, K.J., and Sweet, M.J. (2012). Acute lipopolysaccharide priming boosts inflammasome activation independently of inflammasome sensor induction. Immunobiology *217*, 1325–1329.

Sedger, L.M., Katewa, A., Pettersen, A.K., Osvath, S.R., Farrell, G.C., Stewart, G.J., Bendall, L.J., and Alexander, S.I. (2010). Extreme lymphoproliferative disease and fatal autoimmune thrombocytopenia in FasL and TRAIL double-deficient mice. Blood *115*, 3258–3268.

Silke, J., Rickard, J.A., and Gerlic, M. (2015). The diverse role of RIP kinases in necroptosis and inflammation. Nat. Immunol. *16*, 689–697.

Su, L., Quade, B., Wang, H., Sun, L., Wang, X., and Rizo, J. (2014). A plug release mechanism for membrane permeation by MLKL. Structure *22*, 1489–1500.

Sun, L., Wang, H., Wang, Z., He, S., Chen, S., Liao, D., Wang, L., Yan, J., Liu, W., Lei, X., and Wang, X. (2012). Mixed lineage kinase domain-like protein mediates necrosis signaling downstream of RIP3 kinase. Cell *148*, 213–227.

Sutterwala, F.S., Haasken, S., and Cassel, S.L. (2014). Mechanism of NLRP3 inflammasome activation. Ann. N Y Acad. Sci. *1319*, 82–95.

Varfolomeev, E.E., Schuchmann, M., Luria, V., Chiannilkulchai, N., Beckmann, J.S., Mett, I.L., Rebrikov, D., Brodianski, V.M., Kemper, O.C., Kollet, O., et al. (1998). Targeted disruption of the mouse Caspase 8 gene ablates cell death induction by the TNF receptors, Fas/Apo1, and DR3 and is lethal prenatally. Immunity *9*, 267–276.

Vercammen, D., Beyaert, R., Denecker, G., Goossens, V., Van Loo, G., Declercq, W., Grooten, J., Fiers, W., and Vandenabeele, P. (1998). Inhibition of caspases increases the sensitivity of L929 cells to necrosis mediated by tumor necrosis factor. J. Exp. Med. *187*, 1477–1485.

Vince, J.E., Wong, W.W.L., Gentle, I., Lawlor, K.E., Allam, R., O'Reilly, L., Mason, K., Gross, O., Ma, S., Guarda, G., et al. (2012). Inhibitor of apoptosis proteins limit RIP3 kinase-dependent interleukin-1 activation. Immunity *36*, 215–227.

Wang, H., Sun, L., Su, L., Rizo, J., Liu, L., Wang, L.F., Wang, F.S., and Wang, X. (2014). Mixed lineage kinase domain-like protein MLKL causes necrotic membrane disruption upon phosphorylation by RIP3. Mol. Cell *54*, 133–146.

Welz, P.S., Wullaert, A., Vlantis, K., Kondylis, V., Fernández-Majada, V., Ermolaeva, M., Kirsch, P., Sterner-Kock, A., van Loo, G., and Pasparakis, M. (2011). FADD prevents RIP3-mediated epithelial cell necrosis and chronic intestinal inflammation. Nature *477*, 330–334.

Wilson, N.S., Dixit, V., and Ashkenazi, A. (2009). Death receptor signal transducers: nodes of coordination in immune signaling networks. Nat. Immunol. *10*, 348–355.

Yeh, W.C., de la Pompa, J.L., McCurrach, M.E., Shu, H.B., Elia, A.J., Shahinian, A., Ng, M., Wakeham, A., Khoo, W., Mitchell, K., et al. (1998). FADD: essential for embryo development and signaling from some, but not all, inducers of apoptosis. Science *279*, 1954–1958.

Zhang, J., and Winoto, A. (1996). A mouse Fas-associated protein with homology to the human Mort1/FADD protein is essential for Fas-induced apoptosis. Mol. Cell. Biol. *16*, 2756–2763.

Zhang, J., Cado, D., Chen, A., Kabra, N.H., and Winoto, A. (1998). Fas-mediated apoptosis and activation-induced T-cell proliferation are defective in mice lacking FADD/Mort1. Nature *392*, 296–300.

Zhang, H., Zhou, X., McQuade, T., Li, J., Chan, F.K.M., and Zhang, J. (2011). Functional complementation between FADD and RIP1 in embryos and lymphocytes. Nature *471*, 373–376.

Zhao, J., Jitkaew, S., Cai, Z., Choksi, S., Li, Q., Luo, J., and Liu, Z.G. (2012). Mixed lineage kinase domain-like is a key receptor interacting protein 3 downstream component of TNF-induced necrosis. Proc. Natl. Acad. Sci. USA *109*, 5322–5327.